Effects of fabrication errors on diffraction efficiency for a diffractive membrane

Ruoqiu Wang (王若秋)[1,2], Zhiyu Zhang (张志宇)[1,*], Chengli Guo (国成立)[1,2], Donglin Xue (薛栋林)[1], and Xuejun Zhang (张学军)[1]

[1]*Key Laboratory of Optical System Advanced Manufacturing Technology of the Chinese Academy of Sciences, Changchun Institute of Optics, Fine Mechanics and Physics, Chinese Academy of Sciences, Changchun 130033, China*

[2]*University of Chinese Academy of Sciences, Beijing 100049, China*

**Corresponding author: zhangzhiyu@ciomp.ac.cn*

Received August 22, 2016; accepted October 28, 2016; posted online November 30, 2016

The demand for space-borne telescopes with an aperture of 20 m is forcing the development of large diameter diffractive Fresnel zone lenses (FZLs) on membranes. However, due to the fabrication errors of multi-level microstructures, the real diffraction efficiency is always significantly smaller than the theoretical value. In this Letter, the effects of a set of fabrication errors on the diffraction efficiency for a diffractive membrane are studied. In order to verify the proposed models, a 4-level membrane FZL with a diameter of 320 mm is fabricated. The fabrication errors of the membrane FZL are measured, and its diffraction efficiency in the +1 order is also tested. The results show that the tested diffraction efficiency is very close to the calculated value based on the proposed models. It is expected that the present work could play a theoretical guiding role in the future development of space-borne diffractive telescopes.

OCIS codes: 050.1965, 160.5470, 120.4610.

doi: 10.3788/COL201614.120501.

Recently, there has been an increasing demand for space-borne telescopes to provide geosynchronous-orbit Earth observation capabilities. It is known that the clear aperture of the telescope at Earth's geosynchronous orbit should be as large as 20 m in order to achieve 1-m ground resolution. However, it is almost impossible to develop so large a space-borne telescope with the current reflective optical imaging systems.

Due to their special dispersion characteristics, diffractive optical elements are used in numerous applications today, ranging from spectroscopy, imagination and optical data storage to biomedical applications and even laser material processing (cutting, welding, engraving)[1–6]. A Fresnel zone lens (FZL), which is created by etching a set of concentric rings in an optical substrate, could be used as a diffractive lens to focus light[7]. Moreover, due to their light weight, deployability, and relaxed tolerance, extremely large FZLs fabricated on a thin polyimide membrane are expected to act as the primary lens to build space-based telescopes[8–11].

Low diffraction efficiency is one of the most important drawbacks for FZLs in optical imaging applications. It is well known that the diffraction efficiency of FZLs could be improved by designing a multi-level or quasi-analog surface to approximate a continuous phase distribution[12,13]. However, due to the fabrication complexity of multi-level microstructures, the real diffraction efficiency is always significantly smaller than the theoretical value. For example, although the theoretical diffraction efficiency in the +1 order of a 4-level phase FZL is 81%, Britten *et al.* reported that the diffraction efficiency was only 62% for a 4-level structure on a fused silica substrate with a diameter of 300 mm[14]. When the FZLs' microstructures were transferred onto a polyimide membrane, the diffraction efficiency was reduced to only 55%. Zhang *et al.* also reported that a 4-level primary diffractive membrane with a diameter of 100 mm was achieved with a diffraction efficiency of 52.51%[15].

The reported diffraction efficiency showed a great deviation compared with the theoretical values. The reason behind the loss of the diffraction efficiency has not been sufficiently studied. To the best of our knowledge, several works have analyzed the effects of fabrication errors on the diffraction efficiency of multi-level FZLs on glass[16–19]; however, relatively few works have been published regarding the diffraction efficiency loss for multi-level FZLs on membrane surfaces. In fact, the fabrication errors of membrane FZLs could be classified as master fabrication process (including etching depth errors, overlay registration errors, and linewidth errors) and replication errors (including width transfer errors and depth transfer errors).

In this Letter, based on the theory of scalar diffraction and Fourier optics, the effects of fabrication errors on the diffraction efficiency of membrane FZLs are studied. The mathematical models of diffraction efficiency considering the fabrication errors for a 4-level FZL membrane are obtained. In order to verify the models, a 4-level membrane FZL with a diameter of 320 mm was fabricated. The diffractive microstructures on the membrane surface were measured using a laser scanning confocal microscope (LSCM). The diffraction efficiency in the +1 order was tested. The test results validate the accuracy of the proposed models of fabrication errors.

 © 2016 Chinese Optics Letters

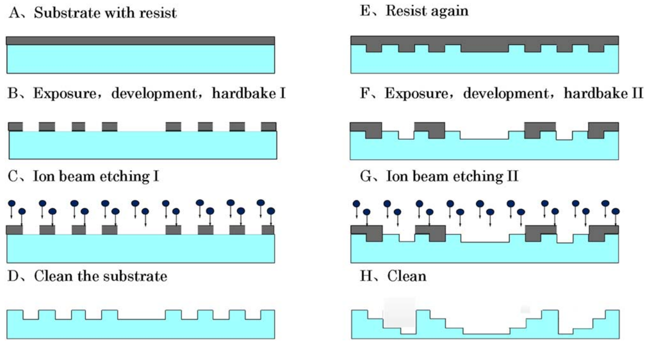

Fig. 1. Process flow for a 4-level master FZL fabrication.

Figure 1 shows a process schematic for the fabrication of the master FZLs on a glass substrate, which has reversed profiles of the designed patterns. The patterns of the first half period are directly written in the photoresist using a mask-less laser lithography system (DWL4000, produced by Heidelberg Instruments, Germany)[20,21]. The system is capable of imaging up to a 400 mm × 400 mm × 48 mm substrate and writing features as small as 0.6 μm. After hardbaking, the photoresist patterns are etched into the fused silica substrate using an Ar-ion beam etching machine (IBF1500, produced by Neue Technologien, Germany)[22]. Using the same processes, the patterns of the other half period are etched into the master substrate with 2 times the depth of the first etching. Finally, a 4-level master FZL is fabricated.

Figure 2 shows the process schematic of the pattern transfer onto the polyimide membrane. The liquid polyimide is cast onto the master FZL and cured to the membrane in place by spin coating, followed by sub-step heating. Spin coating is an effective method to fabricate membranes with good flatness. The liquid polyimide with 2700 cp, and 15% solid content is poured on the master slowly. Then, the polyimide is spin coated at 200 rpm for 10 s and 900 rpm for 110 s onto the membrane with a thickness of approximate 7.5 μm. The experimental temperature and the air humidity are controlled at 22°C and 30% RH, respectively. After spin coating, the master substrate is moved to a heating plate and heated up from 40°C to 70°C at 10°C intervals for 1 h to completely steam out the solvent in the liquid polyimide. Subsequently, the master substrate is put in a vacuum oven at the glass transition temperature of polyimide (350°C) for 1 h to imidize the liquid polyimide into the membrane. It is always necessary to spin coat multiple times to ensure that the membrane has a sufficient thickness.

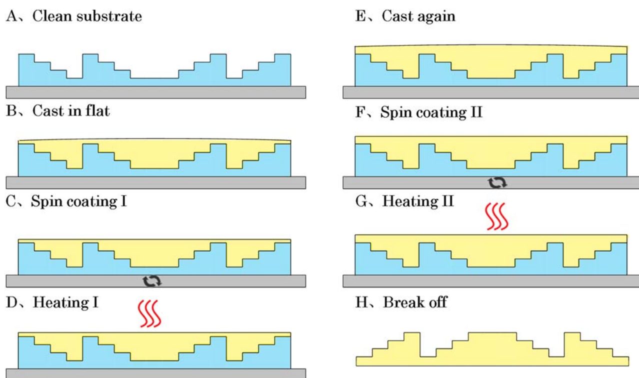

Fig. 2. Process flow for a membrane FZL replication.

Typically, the membrane is first separated from the master substrate, then supported by a circular fixture. Due to the different coefficients of thermal expansion (CTEs) of the fused glass and polyimide, the membrane is in a state of compressive stress when cooling to room temperature. The shrinkage of the membrane occurs because of relaxation when it is separated from the master substrate. Different positions on the membrane were measured, and the results show that the transfer error between the master substrate and the membrane is about 4%. In order to compensate for shrinkage, the membrane must be extended and then fastened. However, it is extremely hard to accurately determine the tension to keep linewidths on the membrane the same as the corresponding ones on the master substrate.

Figure 3 shows an on-substrate prefixing structure, by which the membrane FZL can maintain the horizontal features without linewidth shrinkage. The membrane FZL is first adhered to the fixture, which is made of polyimide, and then separated from glass substrate. The other side of membrane is fastened by an elastic fixture. These fixtures are occluded together by eight symmetrically distributed blocks.

Figure 4 shows the phase distribution of a 4-level diffractive element. It is obvious that the distribution of FZLs is rotationally symmetrical, where r^2 has a periodical distribution at intervals of r_p^2 along the radius. According to the theory of scalar diffraction, when a plane wave with unit amplitude perpendicularly incidents a 4-level diffractive element, the diffracted light field at the image plane can be described as[23]

$$c_m = \frac{1}{T}\int_0^T p(u)\exp(-i2m\pi u/T)\mathrm{d}u, \quad (1)$$

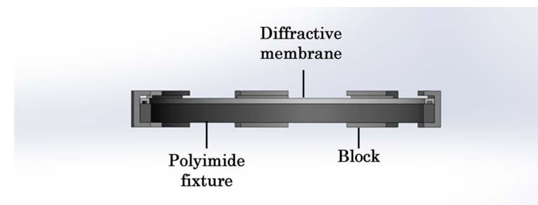

Fig. 3. Schematic of an on-substrate prefixing fixture.

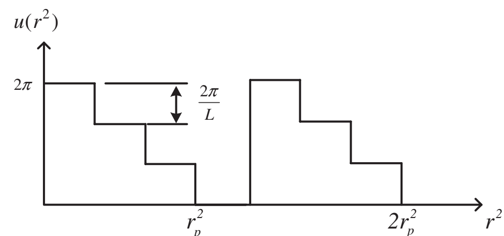

Fig. 4. Phase distribution of a 4-level diffractive element.

where m is the diffractive order, T is the designed width of a cycle band, and $p(u)$ is the transmission function of the diffractive element. For FZLs, the transmission functions have following relations:

$$p(u) = u(x, y) = u(x^2 + y^2) = u(r^2). \quad (2)$$

$u(r^2)$ can be represented by a Fourier series as

$$u(r^2) = \sum_{-\infty}^{+\infty} C_m \exp\left(i2\pi m \frac{r^2}{r_p^2}\right), \quad (3)$$

with Fourier coefficients

$$C_m = \frac{1}{r_p^2}\int_0^{r_p^2} u(r^2)\exp\left(-i2\pi m\frac{r^2}{r_p^2}\right)\mathrm{d}r^2. \quad (4)$$

For a diffractive element without fabrication errors, the transmission function can be expressed as

$$u(r^2) = \sum_{k=0}^{NL-1}\exp\left(\frac{-i2\pi k}{L}\right)\mathrm{rect}\left(\frac{r^2 - kr_p^2/L - r_p^2/2L}{r_p^2/L}\right), \quad (5)$$

where L is the number of phase steps. By normalizing the period value, the amplitude of the mth diffractive order can be expressed as

$$C_m = \int_0^1 \sum_{k=0}^{L-1}\exp\left(\frac{-i2\pi k}{L}\right)\mathrm{rect}\left(\frac{r^2 - k/L - 1/2L}{1/L}\right) \times \exp(-i2\pi r^2)\mathrm{d}r^2$$
$$= \exp\left(-\frac{i\pi m}{L}\right)\sin c\left(\frac{m}{L}\right)\frac{1}{L}\sum_{k=0}^{L-1}\exp\left(-i2\pi\frac{k(m+1)}{L}\right). \quad (6)$$

For a perfect L-level FZL without fabrication errors, the diffraction efficiency η at the +1 order is

$$\eta = |C_{+1}|^2 = \sin c^2\left(\frac{1}{L}\right). \quad (7)$$

The theoretical value of the diffraction efficiency at the +1 order for a 4-level FZL at the +1 order is 81.06%. However, the fabrication errors affect the distribution of the step phase and intensity at the focal point, therefore leading to diffraction efficiency losses. The patterns of the membrane FZLs are replicated from the master FZLs. The major fabrication errors occur both in the fabrication process of the master substrate and the replication process of the membrane.

It is assumed that only etching depth errors exists and are constant over the whole fabrication process, which introduces a constant phase deviation from the designed value. The phase distribution of a 4-level element in a period can be represented in Fig. 5(a), where $\Delta\varphi_1$, $\Delta\varphi_2$, and $\Delta\varphi_3$ are the phase deviations caused by the etching depth errors. The relationships between $\Delta\varphi$ and the etching depth errors can be described as

$$\Delta\varphi_1 = \frac{2\pi}{\lambda}(n-1)d_1, \quad (8)$$

$$\Delta\varphi_2 = \frac{2\pi}{\lambda}(n-1)d_2, \quad (9)$$

$$\Delta\varphi_3 = \Delta\varphi_1 + \Delta\varphi_2, \quad (10)$$

where d_1 and d_2 are the first and second etching depth errors, respectively. Details of the derivation process are included in the Supporting Information. The diffraction efficiency at the +1 order can be described as[19]

$$\eta = |C_{+1}| = \sin c^2\left(\frac{\pi}{4}\right)\frac{\sin c^2(3\pi d_1/2)}{\sin c^2(3\pi d_1/4)}\cos^2\left(\frac{3\pi d_2}{4}\right)$$
$$= \frac{8}{\pi^2}\sin^2\left(\frac{3\pi}{4}d_1\right)\cos^2\left(\frac{3\pi}{4}d_2\right). \quad (11)$$

Assuming that the depth errors are equal in all levels, namely $d_1 = d_2$, the change of the diffraction efficiency with the etching depth errors is shown in Fig. 5(b). It can be seen that when the etching errors reach 10%, the diffraction efficiency is less than 73%.

The phase distribution of a multi-level diffractive element without overlay registration errors is symmetrically circular. However, it's no longer symmetrical when overlay registration errors exist. Assuming that the deviation of the overlay registration is δ, we define $\Delta = \delta/T_j$ to describe the relative overlay registration errors, where T_j represents the interval of adjacent bands, and j is the number of bands ($j = 1, 2, 3\ldots$). Figure 6(a) shows the phase distribution of a 4-level element with overlay registration errors. The relationship between the relative overlay registration errors and the diffraction efficiency can be expressed as[19]

$$\eta = \frac{8}{\pi^2}\left[1 - \sin\left(\frac{\pi|\Delta|}{2}\right)\right]. \quad (12)$$

Figure 6(b) shows the relationship between overlay registration errors and the corresponding diffraction efficiency. The diffraction efficiency is independent of the direction of the overlay registration errors and only related to the absolute value. It can be seen that the diffraction

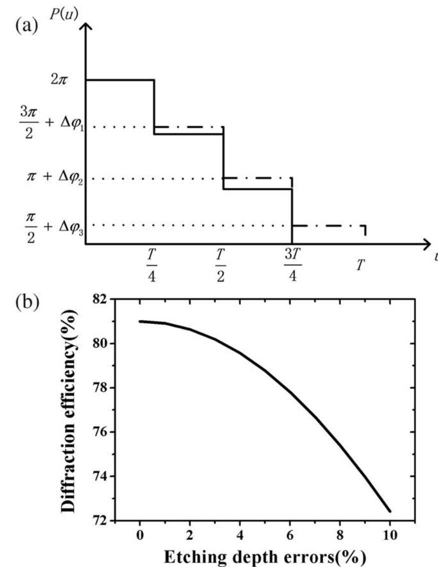

Fig. 5. (a) Phase distribution of a 4-level element with etching depth errors, and (b) relationship between etching depth errors and diffraction efficiency.

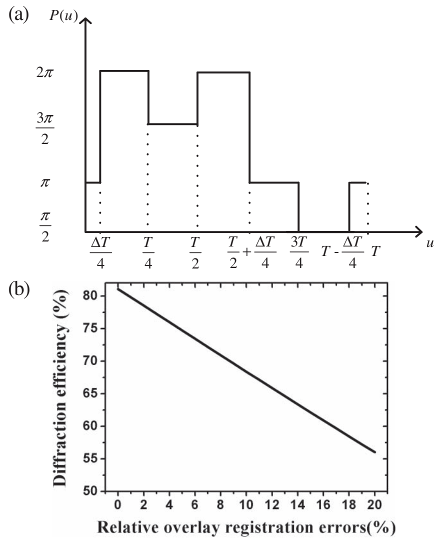

Fig. 6. (a) Phase distribution of a 4-level element with overlay registration errors, and (b) relationship between overlay registration errors and diffraction efficiency.

efficiency decreases linearly along with the increase of the overlay registration errors. In order to obtain a diffraction efficiency larger than 75%, the overlay registration errors need to be controlled within 5%. Therefore, the diffraction efficiency tends to be more susceptible to relative overlay registration errors than etching depth errors.

Assuming that T_1 and T_2 are the desired linewidths, w_1 and w_2 are the linewidth errors. Figure 7(a) shows the phase distribution of a 4-level diffractive element with linewidth errors, where $a_1 = w_1/T_1$ and $a_2 = w_2/T_2$ are the relative linewidth errors in the first and second overlay processes, respectively. The relationship between the relative linewidth errors and diffraction efficiency can be expressed as[19]

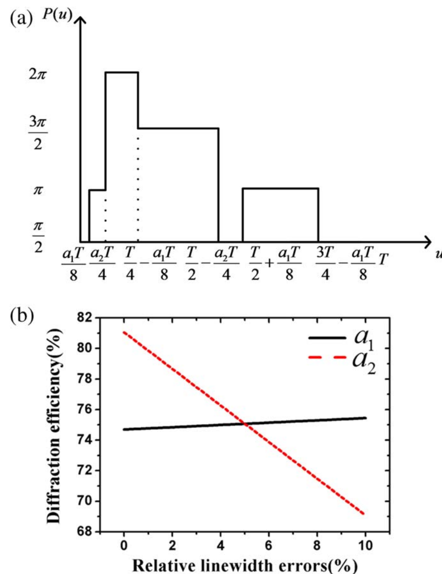

Fig. 7. (a) Phase distribution of a 4-level element with linewidth errors, and (b) relationship between linewidth errors and diffraction efficiency.

$$\eta = \frac{2}{\pi^2}\left(4 - 2\pi a_2 + \frac{3\pi^2 a_1 a_2}{4}\right). \tag{13}$$

Figure 7(b) shows the effect of linewidth errors on diffraction efficiency. The black solid line represents the relationship between a_1 and the diffraction efficiency when $a_2 = 5\%$, while the red dashed line represents the relationship between a_2 and the diffraction efficiency when $a_1 = 5\%$. The relative linewidth errors of a_2 generated in the overlay process have only a slight influence on the diffraction efficiency. However, the relationship between relative linewidth errors a_1 and the diffraction efficiency is linear. A 10% error in the first overlay process leads to a 12% loss of the diffraction efficiency.

Assuming that only width transfer errors exist, the phase distribution of a 4-level element is shown in Fig. 8, where w_t is the width transfer errors, and $a_t = w_t/T$ is the relative width transfer errors. Details of the derivation process are included in the Supporting Information. The diffraction efficiency of a diffractive membrane with transfer width errors can be expressed as

$$\eta = |C_{+1}|^2 = \frac{2}{\pi^2}[1 + 3\cos^2(\pi a_t)]. \tag{14}$$

Assuming that only depth transfer errors exist, the phase distribution of a 4-phase level element is shown in Fig. 9(a), where $\Delta\varphi_t$ is the phase deviation caused by depth transfer errors and is described as

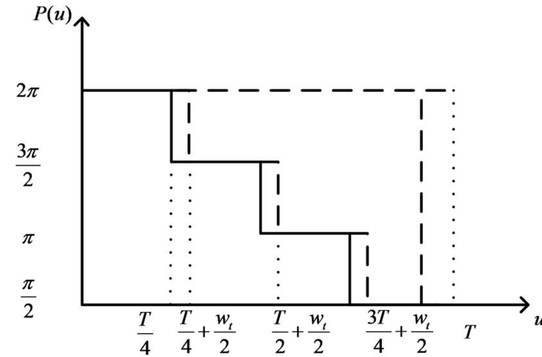

Fig. 8. Phase distribution of a 4-level membrane FZL with width transfer errors.

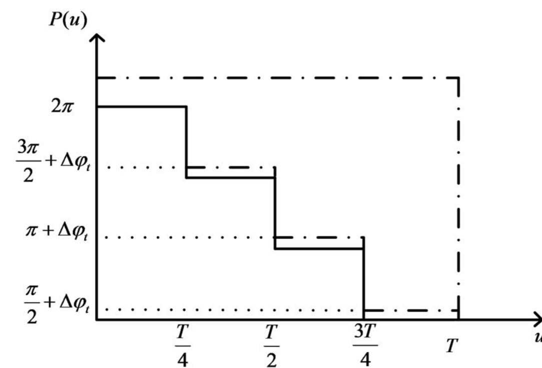

Fig. 9. Phase distribution of a 4-level membrane FZL with depth transfer errors.

$$\Delta\varphi_t = \frac{2\pi}{\lambda}(n-1)d_t. \tag{15}$$

Details of the derivation process are included in the Supporting Information. The diffraction efficiency in the +1 order can be expressed as

$$\eta = |C_{+1}|^2 = \frac{1}{\pi^2}[5 + 3\cos(\Delta\varphi_t)]. \tag{16}$$

The relationship between the transfer errors and the diffraction efficiency is shown in Fig. 10. The black solid line represents the width transfer errors, and the red dashed line represents the depth transfer errors. From the above simulation, it is clear the depth transfer errors are less sensitive than the width transfer errors. When the width transfer errors and depth transfer errors are both 10%, the corresponding diffraction efficiency decreases 4.7% and 3.7%, respectively.

Based on the above-mentioned fabrication processes and prefixing method, a 4-level membrane FZL, as shown in Fig. 11, with a diameter of 320 mm, was fabricated. Figures 12(a) and 12(b) show micrographs of the diffractive microstructures on the membrane surface.

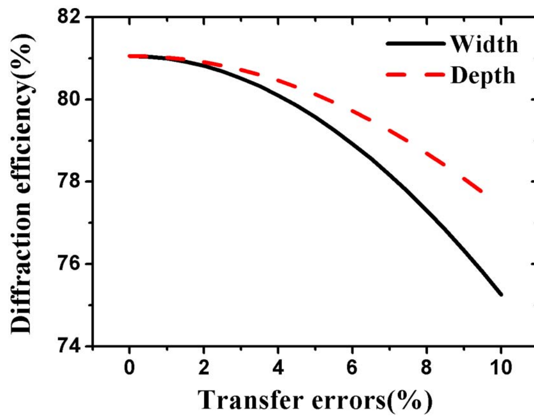

Fig. 10. Relationship between transfer errors and diffraction efficiency.

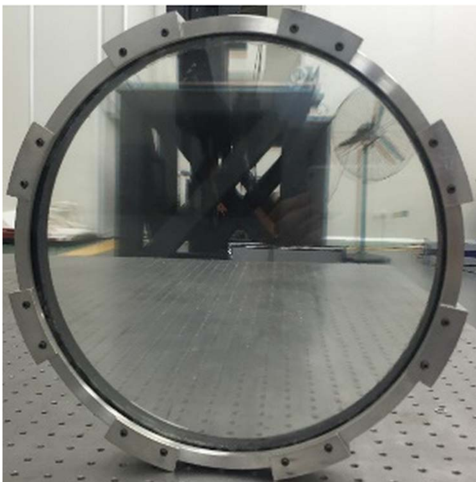

Fig. 11. Photo of 4-step level membrane FZL.

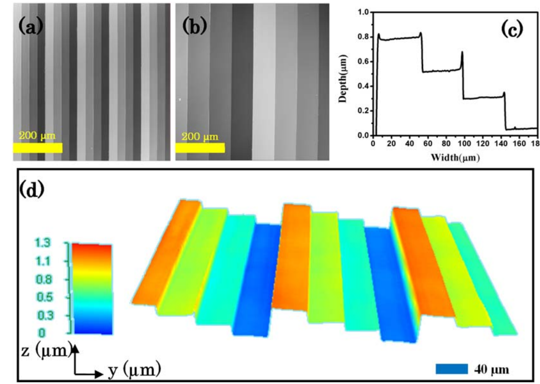

Fig. 12. (a)–(b) Micrographs of two observations in 200× magnification, (c) cross-section profile at the outermost period of diffractive membrane, and (d) 3D scanning result.

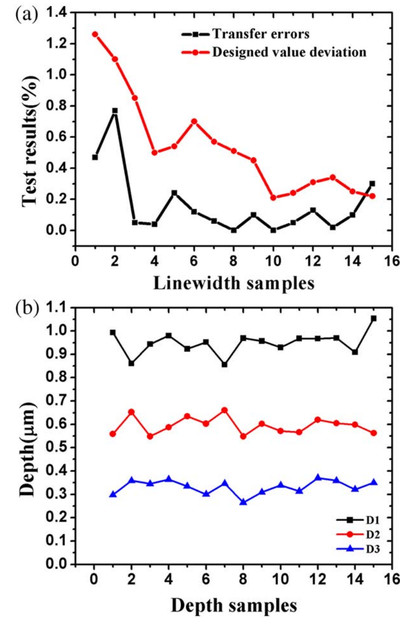

Fig. 13. (a) Linewidths on membrane and (b) test result of each step depth on the membrane.

Figures 12(c) and 12(d) are the surface profile and 3D topography at the outermost period of the membrane FZL, respectively. It is shown that the designed surface profile has completely transferred to the membrane, as evidenced by the sharp edges and steep sidewalls. In order to determine the fabrication errors, the linewidth and step depth in different positions are measured and compared to the corresponding positions on the glass substrate as well as the designed values.

Fig. 14. Distribution map of different diffractive orders.

Table 1. Experimental Data of Diffraction Efficiency

Times	1	2	3	4	5	6	7	8	9	10
E_1/μm	1.880	1.854	1.881	1.780	1.880	1.890	1.800	1.878	1.923	1.879
E_0/μm	2.598	2.670	2.599	2.489	2.60	2.670	2.532	2.60	2.743	2.596
η/%	72.4	69.4	72.4	71.5	72.3	70.8	71.1	72.2	70.1	72.4

Figure 13(a) shows the measured linewidths in different positions. The black line represents the width transfer errors, while the red line represents the deviation from the designed values. It can be seen that the width transfer errors is less than 1%, indicating that the fabrication process and the supported structure are effective at achieving high-precision replications of the master FZL profiles. Figure 13(b) shows the measured results of each step depth in different positions. The depth transfer errors are less than 6%, and the deviation of designed step depth is approximate 10%. It can be concluded that the decrease of the diffractive efficiency loss is mainly introduced by fabrication errors in the master substrate.

Diffraction efficiency η is defined as the light intensity ratio of the primary order E_1 and the incident light E_2, which can be calculated by

$$\eta = \frac{E_1}{E_2}. \tag{17}$$

The diffraction efficiencies of the FZL membrane in different diffractive orders are measured by an He–Ne laser with a 640-nm wavelength. The procedures of the experimental measurements are included in the Supporting Information. The distribution of the different diffractive orders is shown in Fig. 14. The tested diffraction efficiencies of the +1 order are listed in Table 1. By averaging all the measured data, the calculated diffraction efficiency is 71.5%, which is very close to the predicted value of 77.1% based on the proposed model. It is known from our experiments that the most important factor that causes the diffraction efficiency loss is fabrication errors of the master glass, in addition to transfer errors in the replication process. Except for the above-mentioned fabrication errors, measurement errors caused by the system arrangement will also affect the diffraction efficiency:

$$\overline{\eta} = \frac{\sum_{n=1}^{10} \eta_n}{10} = 71.5\%. \tag{18}$$

In conclusion, the relationship between a set of fabrication errors and the overall diffraction efficiency for a 4-level membrane FZL is clarified. By optimizing the fabricating parameters and prefixing the membrane before separating it from the master FZL, we successfully achieve high-precision fabrication of a membrane FZL with a diameter of 320 mm. The measured diffraction efficiency of the membrane FZL is 71.5% at a wavelength of 640 nm, reaching 88% of the theoretical value. The analysis results indicate that the fabrication errors on the glass substrate are the essential factor that causes the diffraction efficiency loss. It is expected that the present work could play a theoretical guiding role in the future development of space-borne diffractive telescopes. The achieved models could also be used in designing large diffractive optics requiring high diffraction efficiency, such as high-power lasers, solar concentrators, and broadband-absorption solar cells.

This work was supported by the National 973 Program of China (No. 2011CB013205) and the National Natural Science Foundation of China (No. 51305422). The authors would like to thank Changchun Hipolyking Co. Ltd. for providing the experimental samples and technical data.

References

1. H. P. Herzig, *Micro-Optics: Elements, Systems and Applications* (Taylor & Francis, 1997).
2. R. A. Hyde, Appl. Opt. **38**, 4198 (1999).
3. J. Early, R. Hyde, and R. Baron, Proc. SPIE **5166**, 148 (2004).
4. W. Qu, H. Gu, and X. Tan, Chin. Opt. Lett. **14**, 031404 (2016).
5. W. Huang, J. Ma, F. Zhu, J. Wang, and C. Zhou, Chin. Opt. Lett. **12**, 070501 (2014).
6. G. Andersen and D. Tullson, Appl. Opt. **46**, 3706 (2007).
7. P. Atcheson, C. Stewart, J. Domber, K. Whiteaker, J. Cole, P. Spuhler, and A. Seltzer, Proc. SPIE **8442**, 10 (2012).
8. I. M. Barton, J. A. Britten, S. N. Dixit, L. J. Summers, I. M. Tomas, M. C. Rushford, K. Lu, R. A. Hyde, and M. D. Perry, Appl. Opt. **40**, 4 (2001).
9. J. L. Domber, P. D. Atcheson, and J. Kommers, in *Spacecraft Structures Conference* (2014).
10. P. Atcheson, J. Domber, K. Whiteaker, J. A. Britten, S. N. Dixit, and B. Farmer, Pro. SPIE **9143**, 91431 (2014).
11. M. Rahlves, M. Rezem, K. Boroz, S. Schlangen, E. Reithmeier, and B. Roth, Opt. Express **23**, 3 (2015).
12. J. C. Feltz, Opt. Eng. **29**, 893 (1990).
13. A. B. Meinel and M. P. Meinel, Opt. Eng. **41**, 8 (2002).
14. A. B. Jerald and M. P. Meinel, Appl. Opt. **53**, 11 (2014).
15. Y. Zhang and B. Wang, Proc. SPIE **9622**, 96220G (2015).
16. F. Margit, K. Berndt, and E. Pawlowski, Opt. Eng. **33**, 33 (1994).
17. S. Wang, W. Yang, and S. B. Wu, Proc. SPIE **8911**, 89110O (2013).
18. M. B. Stern, M. Holz, S. S. Medeiros, and R. E. Knowlden, J. Vac. Sci. Technol. **9**, 3117 (1991).
19. G. F. Jin, Y. B. Yan, and M. X. Wu, *Binary Optics* (Publishing House of National Defence Industry, 1998).
20. A. Y. Smuk and N. M. Lawandy, Opt. Lett. **22**, 1030 (1997).
21. C. Liu, X. Guo, F. Gao, B. Luo, X. Duan, J. Du, and C. Qiu, Proc. SPIE **5645**, 307 (2005).
22. T. Haensel, A. Nickel, and A. Schindler, in *Optical Fabrication & Testing* (2008).
23. M. Born and E. Wolf, *Principles of Optics* (Mathematical Gazette, 1975).